ELSEVIER

Biophysical Chemistry 134 (2008) 72–83

Biophysical Chemistry

http://www.elsevier.com/locate/biophyschem

# DNA binding and photocleavage properties of a novel cationic porphyrin-anthraquinone hybrid

Ping Zhao [a], Lian-Cai Xu [a], Jin-Wang Huang [a,b,*], Kang-Cheng Zheng [a], Jie Liu [a], Han-Cheng Yu [a], Liang-Nian Ji [a,b,c]

[a] *MOE Laboratory of Bioinorganic and Synthetic Chemistry, School of Chemistry and Chemical Engineering, Sun Yat-Sen University, Guangzhou 510275, PR China*

[b] *State Key Laboratory of Optoelectronic Material and Technologies, Sun Yat-Sen University, Guangzhou 510275, PR China*

[c] *The Key Laboratory of Gene Engineering of Ministry of Education, Sun Yat-Sen University, Guangzhou 510275, PR China*

Received 9 November 2007; received in revised form 19 January 2008; accepted 19 January 2008
Available online 9 February 2008

**Abstract**

A novel cationic porphyrin-anthraquinone (Por-AQ) hybrid has been synthesized and characterized. Using the combination of absorption titration, fluorescence spectra, circular dichroism (CD) as well as viscosity measurements, the binding properties of the hybrid to calf thymus (CT) DNA have been investigated compared with its parent porphyrin. The experimental results show that at low [Por]/[DNA] ratios, the parent porphyrin binds to DNA in an intercalative mode while the hybrid binds in a combined mode of outside binding (for porphyrin moiety) and partial intercalation (for anthraquinone). Ethidium bromide (EB) competition experiment determined the binding affinity constants ($K_{app}$) of the compounds for CT DNA. Theoretical calculational results applying the density functional theory (DFT) can explain the different DNA binding behaviors reasonably. $^1O_2$ was suggested to be the reactive species responsible for the DNA photocleavage of porphyrin moieties in both two compounds. The wavelength-depending cleavage activities of the compounds were also investigated.


*Keywords:* Porphyrin-anthraquinone hybrid; DNA binding; DFT calculations; DNA photocleavage; Wavelength-depending

## 1. Introduction

Cationic porphyrins, represented by *meso*-tetra(*N*-methylpyridinium-4-yl)porphyrin (TMPyP), have been considered as bifunctional compounds for their marked photochemical nuclease activities [1,2] and tight interactions with DNA through different binding modes [3–11]. This double functionality can be influenced by conjugation of the cationic porphyrin motif and another structure unit which also, by itself, can interact with DNA. A variety of these structural units, such as nucleotide [12], acridine [13] and phenylpiperazine [14], have been designed and introduced at the *meso*-20-position of TMPyP-like porphyrins, respectively. Among the various chromophores that can be used to link to the porphyrin, anthraquinone seems to be an ideal candidate because this ubiquitous electron acceptor has been established to be an avid binder and also an efficient photocleavage agent of DNA [15–17]. Despite many reports on the electron-transfer and the light-induced nuclease activity of non-charged porphyrin-anthraquinone (Por-AQ) hybrids [18–22], so far no studies on the conjugation of cationic porphyrin with anthraquinone as well as the interaction of such Por-AQ hybrids with DNA were reported. Since cationic porphyrins have higher DNA affinities than non-charged porphyrins for their extra electrostatic effect with the negative phosphate groups of DNA backbone [3–11], it is expected that the novel cationic porphyrin-anthraquione hybrid will show a better DNA binding ability and photocleavage activity than its neutral analogues. Moreover, since anthraquione is an effective DNA cleavage reagent and has a different excitation wavelength from porphyrin, the introduction of

* Corresponding author. MOE Laboratory of Bioinorganic and Synthetic Chemistry, School of Chemistry and Chemical Engineering, Sun Yat-Sen University, Guangzhou 510275, PR China. Tel.: +86 20 84113317; fax: +86 20 84112245.

*E-mail address:* ceshjw@163.com (J.-W. Huang).

0301-4622/$ - see front matter © 2008 Elsevier B.V. All rights reserved.
doi:10.1016/j.bpc.2008.01.009

anthraquione group to the cationic porphyrin is supposed to increase the wavelength selectivity of DNA photocleavage in comparison with the porphyrin alone.

On the other hand, the interaction of small molecules with DNA has attracted many theoretical chemists in recent years. Various theoretical researchers have been trying to correlate some theoretical predictions to the experimental findings of the DNA binding behaviors. However, at present, the full supramolecular system formed from DNA and a ligand is too large in size to be calculated using the quantum-chemical method. Thus, it is very important and necessary to theoretically analyze the interaction between ligands and DNA from their individual electronic structural characteristics and explore the trend in DNA-binding affinities of ligands and related behaviors. DFT calculations, which can better consider the electronic correlation energy and obviously reduce the computational expenses, have been broadly applied to this field [23,24]. Kurita and Kobayashi [25] have reported the density functional MO (molecular orbital) calculations for stacked DNA base-pair model, and their calculated results show that the energies of the HOMO (the highest occupied molecular orbital) and these occupied MOs near HOMO are rather high and their components are mainly distributed on the base pairs of DNA. Therefore, Kurita's results offered a theoretical foundation for the base pairs of DNA being good electron donors. We have also reported some DFT results on the electronic structures and related properties of some Ru (II) polypyridyl complexes and successfully discussed their DNA-binding trend and related properties [26–29]. These theoretical efforts are significant in guiding experimental works. Although some DFT calculation results on porphyrin have been reported [30,31], so far the theoretical reports on Por-AQ hybrids and the theoretical explanation on their DNA binding behaviors have not been found yet.

In this paper, we report the synthesis and characterization of a novel cationic Por-AQ hybrid, 5-[4-[(1-*N*-anthraquinonon-yl) acetyloxohydroxyl]phenyl]-10, 15, 20-tris(*N*-methylpyridinium-4-yl)porphyrin triiodide ([AQATMPyP]$I_3$), in which a 1-amino-9,10-anthraquinone is attached to the *para* position of the phenyl in tricationic porphyrin with an acetyl (Fig. 1). Moreover, its parent porphyrin, 5-hydroxyphenyl-10, 15, 20-tris (*N*-methylpyridinium-4-yl)porphyrin triiodide ([HTMPyP]$I_3$), is also presented for comparison (Fig. 1). The main purpose of this paper is to reveal the DNA binding and photocleavage behaviors of such an interesting Por-AQ hybrid. At the same time, the theoretical calculations applying DFT were also carried out to explain the DNA binding properties. The DNA photocleavage mechanism and wavelength-depending cleavage activities of these two compounds were also comparably investigated.

## 2. Experimental

### 2.1. Materials and chemicals

The precursor HTPyP, 5-(4-hydroxyphenyl)-10, 15, 20-tris(4-*N*-pyridiniumyl)porphyrin, was synthesized according to [32]. 5-[4-[(1-*N*-anthraquinonon-yl)acetyloxohydroxyl]phenyl]-10, 15, 20-trisphenylporphyrin (AQATPP), was previously synthesized in our laboratory [22]. 1-amino-9, 10-anthraquinone (Sigma), bromoacetic acid (Sigma), silica gel (Qingdao) and chloroform (Guangzhou) were commercially available and of analytical grade. CT DNA, pBR322 supercoiled plasmid DNA was obtained from the Sigma Company. Tris buffer I (Tris = Tris(hydroxymethyl)aminomethane) for absorption titration, emission, CD as well as viscosity experiments contains 5 mM Tris–HCl, 50 mM NaCl (pH = 7.2). Tris buffer II for the gel electrophoresis experiment contains 50 mM Tris–HCl, 18 mM NaCl (pH = 7.2). A solution of CT DNA in the buffer gave a ratio of UV absorbance at 260 and 280 nm of 1.85:1, indicating that the DNA was sufficiently free of protein. The DNA concentration per nucleotide was determined by absorption spectroscopy using the molar absorption coefficient (6600 $M^{-1}$ $cm^{-1}$) at 260 nm [33].

### 2.2. Measurements

Element analysis (C, H, and N) was carried out with a Perkin-Elmer 240 Q elemental analyzer. $^1$H NMR spectra were recorded on a Varian-300 spectrometer. All chemical shifts are given relative to tetramethylsilane (TMS). Electrospray mass spectra (ES-MS) were recorded on a LCQ system (Finnigan MAT, USA). UV–Vis spectra were recorded on a Perkin-Elmer-

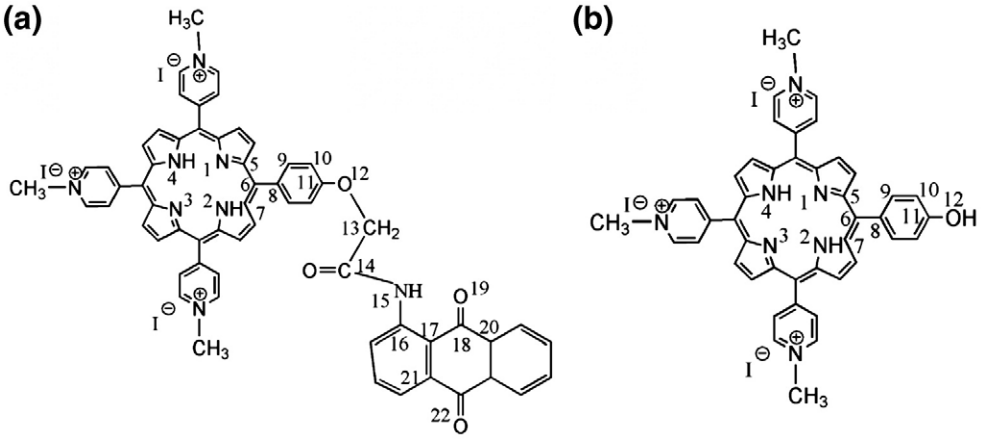


Fig. 1. Structural schematic diagrams of [AQATMPyP]$I_3$ (a) and [HTMPyP]$I_3$ (b).

Lambda-850 spectrophotometer. Emission spectra were recorded on a Perkin-Elmer L55 spectrofluorophotometer. CD spectra were recorded on a JASCO-J810 spectrometer. Viscosity measurements were carried out with an Ubbelohde viscometer maintained at a constant temperature of (30±0.1) °C in a thermostatic bath. Flow time was measured with a digital stopwatch. For the gel electrophoresis experiment, a high pressure mercury lamp-light filter assembly was used. Yellow light filter was used for visible light ($\lambda > 470$ nm) and purple filter for ultraviolet light ($\lambda < 350$ nm). The samples were analyzed by electrophoresis for 1 h at 120 V in Tris-acetate buffer containing 1% agarose gel. The gel was stained with 1 μg $ml^{-1}$ ethidium bromide and photographed under UV light. Cyclic voltammetry (CV) measurements used a three-electrode cell configuration consisting of a platinum working electrode, a silver ($Ag/Ag^+$) reference electrode, and a platinum auxiliary electrode. The supporting electrolyte was 0.1 M tetrabutyl ammonium perchorate (TEAP) buffered at pH=7 which had been $N_2$ purged to remove molecular oxygen. The values obtained were normalized with respect to the normal hydrogen electrode (NHE).

### 2.3. Theoretical detail

The full geometry optimization computations of [AQATMPyP]$I_3$ and [HTMPyP]$I_3$ were carried out with the DFT-B3LYP method and 6-31G basis set and there is not any symmetry appearing in these two compounds. In order to vividly depict the details of the frontier molecular orbital interactions, the stereographs of some related frontier molecular orbitals of the complexes were drawn with the Molden v 4.2 program [34] based on the computational results. All calculations were performed with the G03 (d01) program-package [35].

### 2.4. Synthesis

#### 2.4.1. [HTMPyP]$I_3$

A mixture of HTPyP [16] (1 mmol, 0.63 g) and methyl iodide (120 equiv) were refluxed in dry $CHCl_3$ for 8 h at room temperature. The reaction was monitored by TLC with a mixture of $CH_2C1_2$–EtOH (95/5) as eluant (the final product does not migrate on TLC). The solvent and the excess of methyl iodide were removed under vacuum. The residue was dissolved in methanol and precipitated with diethylether to yield the cationic porphyrin [HTMPyP]$I_3$ in quantitative yields. Yield: 1.03 g, 95.4% (Found: C, 48.83; H, 3.56; N, 9.88%. Calc. for $C_{44}H_{36}I_3ON_7 \cdot 2H_2O$: C, 48.92; H, 3.55; N, 9.93). ES-MS [EtOH, m/z]: 678 ($[HTMPyP]^+$), 339($[HTMPyP]^{2+}$), 226 ($[HTMPyP]^{3+}$). $^1$H NMR (300 MHz, DMSO): chemical shift δ: 9.448(d, J=5.94 Hz, 6H, 2, 6-pyridinium), 9.12(s, 4H, β-pyrrole), 9.05(s, 4H, β-pyrrole), 8.978(d, J=5.51 Hz, 6H, 3, 5-pyridinium), 8.00(d, J=8.13 Hz, 2H, 2, 6-phenyl), 7.255(d, J=8.06 Hz, 2H, 3, 5-phenyl), 4.711(s, 9H, $N^+$–Me), 3.00(s, 1H, OH), −2.957(s, 2H, NH pyrrole).

#### 2.4.2. BMAAQ (Bromomethoxylamino-anthraquinone)

Bromoacetic acid (10 mmol, 1.5 g) was dissolved in 35 mL of thionyl chloride and the solution was refluxed for 2 h. After cooling to room temperature, thionyl chloride was removed under reduced pressure. Dry benzene (30 mL) was used to wash the residue and then removed. To this residue, a solution of 1-amino-9, 10-anthraquione (5 mmol, 1.1 g) dissolved in dry benzene was added and then the reaction mixture was refluxed for 4 h. The solvent then removed under reduced pressure. BMAAQ was then gained after washing with 5% $Na_2CO_3$. Yield: 1.55 g, 90%. ES-MS [EtOH, m/z]: 342($BMAAQ^+$).

#### 2.4.3. [AQATMPyP]$I_3$

A mixture of HTPyP [16] (0.15 mmol, 0.095 g), BMAAQ (0.3 mmol, 0.102 g) and anhydrous $K_2CO_3$ (0.7 g) in DMF (20 mL) was stirred for 48 h at room temperature. Then the reaction mixture was poured into water (50 mL) and filtered. The crude material was extracted by a mixture of $CHCl_3$–EtOH (25/1, v/v) and purified by chromatography. Evaporation of solvent afforded 200 mg of 5-[4-[(1-*N*-anthraquinonon-yl) acetyloxohydroxyl]phenyl]-10, 15, 20-tris(4-pyridiniumyl)-porphyrin (AQATPyP) as a purple powder (6–7%). AQATPyP was then methylated with the same method as HTPyP does and yielded the cationic porphyrin [AQATMPyP]$I_3$ in quantitative yields. Yield: 0.121 g, 92% (Found: C, 53.38; H, 3.64; N, 8.67%. Calc. for $C_{60}H_{47}I_3O_4N_8 \cdot 4H_2O$: C, 53.44; H, 3.66; N, 8.73%). ES-MS [EtOH, m/z]: 941 ($[AQMTPyP]^+$), 470($[AQMTPyP]^{2+}$), 339 ($[AQATMPyP]^{3+}$). $^1$H NMR (300 MHz, DMSO): chemical shift δ 12.591 (s, 1H, NH–C=O), 9.492(d, J=5.92 Hz, 6H, 2, 6-pyridinium), 9.139(s, 4H, β-pyrrole), 9.043(d, J=4.50 Hz, 4H, β-pyrrole), 8.950(s, 6H, 3,5-pyridinium), 8.392(d, J=5.92 Hz, 2H, 2, 6-phenyl), 8.014(s, 2H, 3,5-phenyl), 7.785(d, J=6.53 Hz, 4H, AQ-phenyl), 7.089(s, 2H, AQ-phenyl), 5.089(s, 1H, AQ-phenyl), 4.725(s, 9H, $N^+$–Me), −3.278(s, 2H, NH pyrrole).

## 3. Results and discussion

### 3.1. DNA-binding properties

#### 3.1.1. Absorption titrations

The absorption spectra of [AQATMPyP]$I_3$ and [HTMPyP]$I_3$ in the absence and presence of increasing amounts of CT DNA are given in Fig. 2. Both compounds exhibit an intense absorption band around 420 nm and four weak bands around 550 nm, which are attributed to porphyrin ring, namely Soret band and Q bands, respectively [3,4,36]. As to [AQATMPyP]$I_3$, another intense absorption band centered at 250–300 nm, which can be attributed to the anthraquinone moiety of the hybrid, is also clearly observed. The titration of DNA induces large spectral perturbations in the porphyrin's Soret bands of both two compounds. The hypochromism and bathochromism reach 48.68%, 6 nm and 47.49%, 13 nm for [AQATMPyP]$I_3$ (Fig. 2a) and [HTMPyP]$I_3$ (Fig. 2b), respectively.

The magnitude of spectral perturbation is an intuitional evidence for DNA binding [2,4]. As is well known, intercalation of porphyrin into DNA base pairs is characterized by a red shift (>10 nm) and intensity decrease (up to 40%) in the Soret band of UV–Vis spectra; groove binding mode shows no (or minor) change in UV–Vis spectra while outside binding mode also exhibits red shift and intensity decrease in the Soret band of

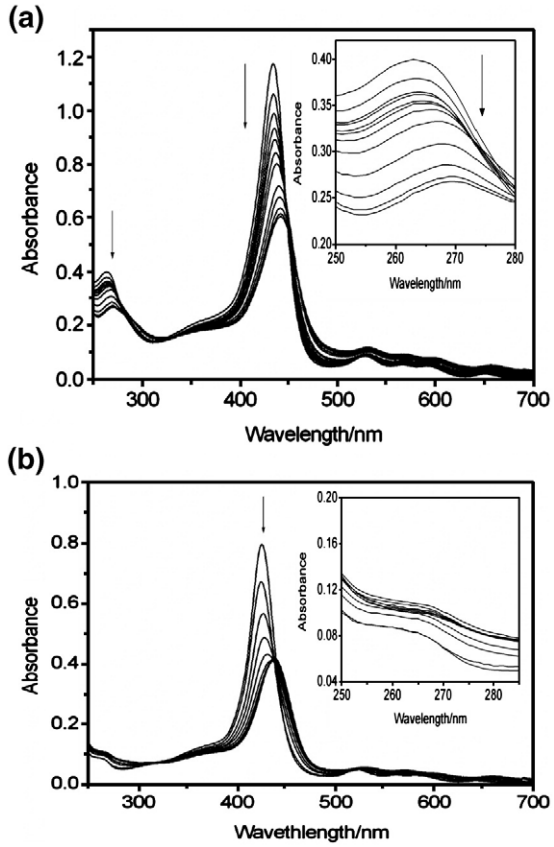


Fig. 2. Absorption spectra of $[AQATMPyP]I_3$ (a) and $[HTMPyP]I_3$ (b) in Tris buffer (pH = 7.2, 0.05 M NaCl) at 25 °C in the presence of increasing amounts of CT DNA. [Por] = 10 μM. Arrows indicate the change in absorbance upon increasing the DNA concentration. Inset: absorption spectra at 250–280 nm.

porphyrins [4–6,10,37,38]. Thus, the large degree of hypochromism and bathochromism of $[HTMPyP]I_3$ is a sign of the intercalative binding mode. Although the hypochromism extent of $[AQATMPyP]I_3$ is almost the same as its parent porphyrin, the bathochromism of the Soret band is only 6 nm, and thus it may interact with DNA in outside binding mode. It should be reasonable to propose that the induction of anthraquinone moiety brings about steric hindrance to the cationic porphyrin and thus changes its binding mode.

We also monitored the absorbance change of $[AQATMPyP]I_3$ and $[HTMPyP]I_3$ at the range of 250–280 nm which is the characteristic absorption of anthraquinone moiety (Fig. 2, insert). In the case of $[AQATMPyP]I_3$, a peak with large hypochromism and bathochromism (reaching 33.2% and 7 nm) is observed. On the contrary, the absorbance of $[HTMPyP]I_3$ at this range is rather low, with no obvious shift or hypochromism (hyperchromism). This indicates that the influence of increasing DNA in the system is negligible [33]. Thus, the large spectral perturbation of $[AQATMPyP]I_3$ at this range is evidently induced by the intense interaction between the anthraquinone moiety and DNA. Due to its excellent planarity and the hindrance results from the cationic porphyrin moiety which binds to DNA in outside mode, we propose that the anthraquinone plane may bind to DNA in partial intercalative mode.

### 3.1.2. Fluorescence studies

The results of emission titration for $[AQATMPyP]I_3$ and $[HTMPyP]I_3$ with DNA are illustrated in Fig. 3. Emission peak at *ca.* 660 nm, which is the characteristic emission peak of porphyrin chromophore, is observed to increase for both compounds with the increase of DNA. The fluorescence intensity of $[AQATMPyP]I_3$ (Fig. 3a)at *ca*. 660 nm is much weaker than that of its parent porphyrin, which can be explained by the occurrence of a photoinduced-electron-transfer (PET) reaction from the porphyrin singlet state to the appended anthraquinone [39]. Another intense emission peak at *ca.* 370 nm, which can be ascribed to the anthraquinone moiety in the hybrid, is clearly observed to increase for $[AQATMPyP]I_3$ (Fig. 3a, insert). The increase in emission intensities of the compounds most probably result from the interaction between the small molecules and DNA, since the hydrophobic environment provided by DNA reduces the accessibility of water molecules to the compound and the mobility of the compound is restricted at the binding site, leading to a decrease in radiationless vibrational relaxation [40]. The increases in both porphyrin's and anthraquinone's emission ranges also suggest that both two moieties in the hybrid interact with DNA rather strongly.

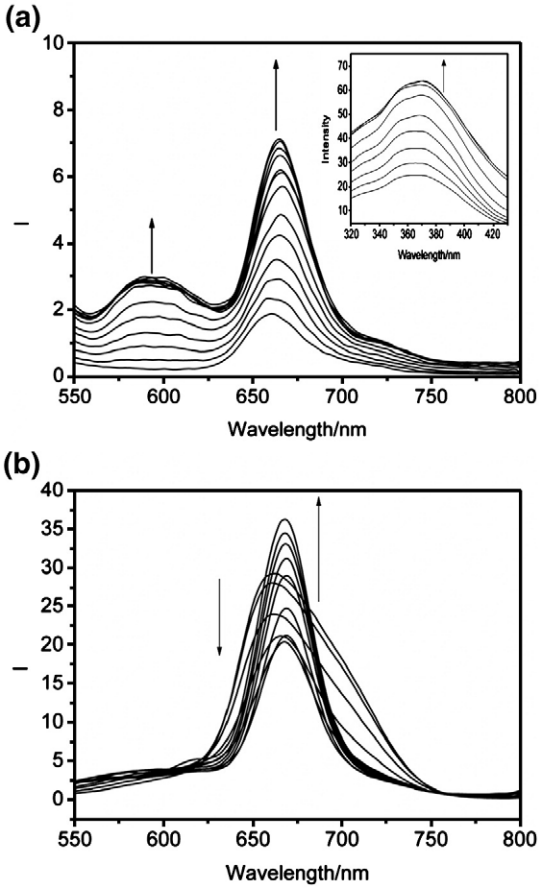


Fig. 3. Emission spectra of $[AQATMPyP]I_3$ (a) and $[HTMPyP]I_3$ (b) in Tris buffer (pH = 7.2, 0.05 M NaCl), in the absence and presence of CT DNA. [Por] = 10 μM. Arrows show the intensity change upon increasing DNA concentrations. $\lambda_{exc}$ = 448 nm for $[AQATMPyP]I_3$ and 437 nm for $[HTMPyP]I_3$ (Inset: the emission of $[AQATMPyP]I_3$ excited at 263 nm).

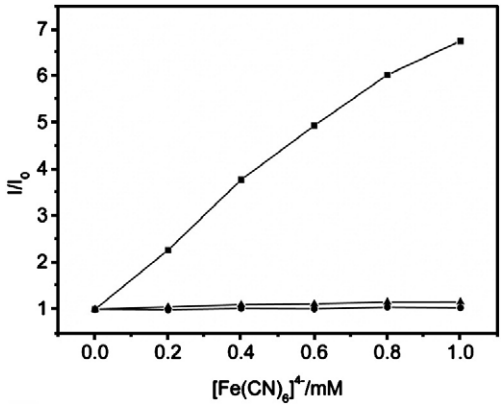


Fig. 4. Emission quenching with $[Fe(CN)_6]^{4-}$ for free (■) or DNA-bound (▲) $[HTMPyP]I_3$ and DNA-bound (●) $[AQATMPyP]I_3$ in Tris buffer (pH = 7.2, 0.05 M NaCl) [Por]/[DNA] = 0.025.

In Fig. 3b, it is notable that the fluorescence intensity of $[HTMPyP]I_3$ decreases upon the addition of a low concentration of DNA ([Por]/[DNA] ≥ 0.94), which may result from self-stacking of the free base porphyrin along the DNA surface. This self-stacking of $[HTMPyP]I_3$ in the presence of a small amount of DNA is a result of the proximity of the neighbouring porphyrin molecules to each other. However, at higher concentrations of DNA, the emission intensity of $[HTMPyP]I_3$ begins to increase. The increased fluorescence emission in excess amounts of DNA can be attributed to the reduced self-stacking of the porphyrin molecules and their subsequent intercalation into the DNA bases. Similar phenomenon is also observed for TMPyP [41–43]. However, no obvious decrease in the fluorescence emission intensity of $[AQATMPyP]I_3$ is observed, which indicates that the steric hindrance brought by anthraquinone reduces the porphyrin-moiety's self-stacking.

Steady-state emission quenching experiments using potassium ferrocyanide ($K_4Fe(CN)_6$) as a quencher were also used to observe the binding of porphyrin compounds to CT DNA. As shown in Fig. 4, in the absence of DNA, the fluorescence of $[HTMPyP]I_3$ is efficiently quenched by $[Fe(CN)_6]^{4-}$, resulting in an almost linear Stern–Volmer plot with a slope of 6.7. In the case of $[AQATMPyP]I_3$, its fluorescence is completely quenched in the absence of DNA since its fluorescence is very weak. However, the addition of DNA makes the slopes of the two compounds drastically decreased to almost zero. This behavior may be explained by the repulsion of the highly anionic $[Fe(CN)_6]^{4-}$ by the DNA polyanion which hinders the bound compound from quenching of the emission. The slope reflects different degrees of protection or relative accessibility of bound cations and can be taken as a measure of binding affinity [44]. Since a smaller slope corresponds to better protection and stronger binding affinity, both two compounds should bind to the DNA rather strongly, based on the experimental results.

### 3.1.3. CD studies

The CD spectra experiment may be one of the most direct means of examining the binding modes of the porphyrin compounds to DNA. In the visible range, the porphyrins alone as well as the DNA by themselves do not show any ellipticity. However, an induced CD spectrum is obtained if there is a binding between the porphyrin and the DNA. The sign of the induced CD spectrum in the Soret region can be used as a sensitive signature for the binding modes of porphyrins to DNA: a positively induced CD band is an indication of groove binding, a negatively induced CD band is produced upon intercalation and a conservative, bisignal induced CD band is the characteristic of outside binding [4,5,7].

Fig. 5 illustrates the induced CD spectra for porphyrins bound to CT DNA in [Por]/[DNA] ratio ranged from 0.4 to 0.05. None of these two porphyrins as well as DNA by themselves displays any CD spectra signal in the visible region, but induced CD spectra are observed in the Soret band of the two porphyrins with DNA titration. The ellipticity observed for $[HTMPyP]I_3$ in the presence of DNA is predominantly negative in character and centered at the wavelength range from 430 to 470 nm. With the increasing concentration of DNA, the negative signal of CD spectrum becomes stronger. Since the

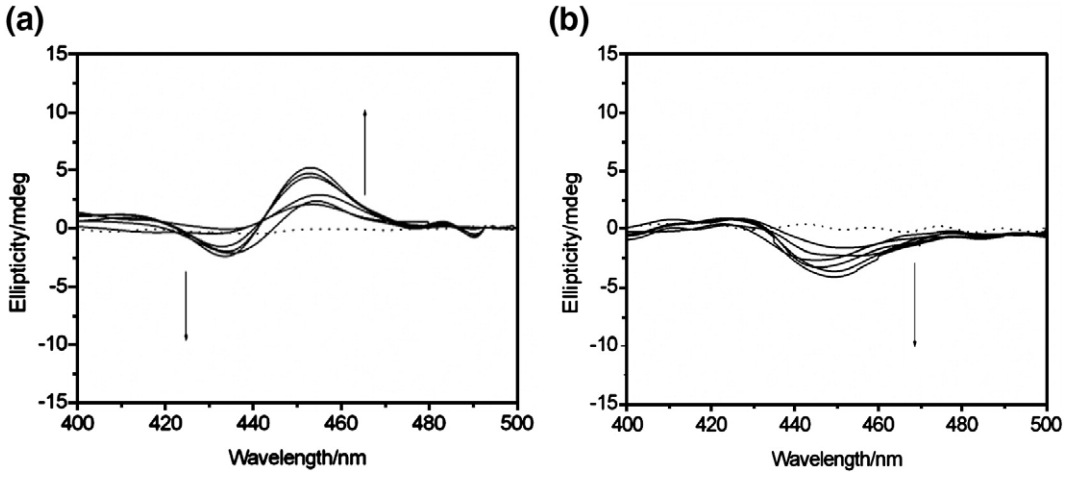


Fig. 5. Induced CD spectra of $[AQATMPyP]I_3$ (a) and $[HTMPyP]I_3$ (b) in the absence (dot line) and presence (solid line) of CT DNA in Tris buffer (pH = 7.2, 0.05 M NaCl). [Por] = 10 μM. [Por]/[DNA] = 0.4, 0.3, 0.2, 0.15, 0.10, 0.05. Arrows indicate the change in CD spectra upon increasing the DNA concentration.

negative CD signal is diagnostic of intercalative binding, this result confirms that [HTMPyP]$I_3$ intercalates into the DNA duplex under the experimental conditions. In the case of [AQATMPyP]$I_3$, at lower DNA concentrations([Por]/[DNA]≥0.3), the porphyrin moiety in the hybrid displays a positive peak centered around 453 nm, which indicates that the porphyrin binds to DNA in an groove binding mode initially. However, the increase in DNA concentration results in the development of a negative peak centered around 434 nm, and meanwhile the positive peak becomes stronger. The appearance of conservative CD spectra indicates that the binding mode of the porphyrin moiety changes from groove binding mode to outside binding mode. The distinct CD signals of two compounds are in good consistent with foregoing experimental results.

### 3.1.4. Viscosity

In the absence of X-ray structural data, hydrodynamic methods which are sensitive to changes in the length of DNA are arguably the most critical test of the classical intercalation model, and therefore they provide the most definitive means of inferring the binding mode of DNA in solution [4]. Intercalation mode is expected to lengthen the DNA helix as the base pairs are pushed apart to accommodate the bound ligand, leading to an increase in the DNA viscosity. In contrast, a partial, non-classical intercalation of ligand could bend (or kink) the DNA helix and reduce its effective length and, concomitantly, its viscosity. When outside binding or groove binding occurs, the viscosity of DNA will not change basically [3,4,38,45,46].

The viscosity of the buffer solutions of CT DNA increases with the addition of [HTMPyP]$I_3$ (Fig. 6). Such an increase provides striking evidence for the intercalation of [HTMPyP]$I_3$ into the DNA duplex. However, in the case of [AQATMPyP]$I_3$, the relative viscosity of DNA is remarkably decreased with the increasing addition of the hybrid. CD spectra have confirmed that the porphyrin moiety in [AQATMPyP]$I_3$ binds to DNA with outside binding mode (or groove binding mode) which will not change viscosity basically. Thus, the decrease in the viscosity of DNA can be ascribed to the partial intercalation of anthraquinone plane to DNA duplex. However, it is very interesting that the decrease in the viscosity of DNA with the increase in concentration of [AQATMPyP]$I_3$ is amazingly quick.

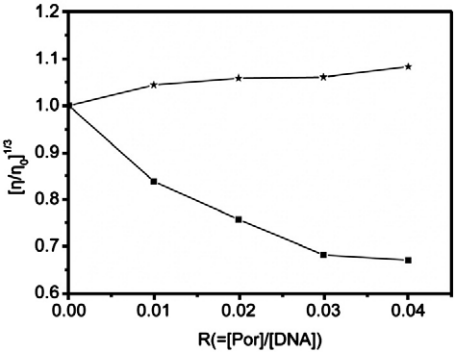


Fig. 6. Plots of the relative viscosity of CT DNA (0.5 mM) *vs.* R value of [AQATMPyP]$I_3$ (■) and [HTMPyP]$I_3$ (★) in phosphate buffer (pH=7.2, 0.05 M NaCl) at (30±0.1)°C.

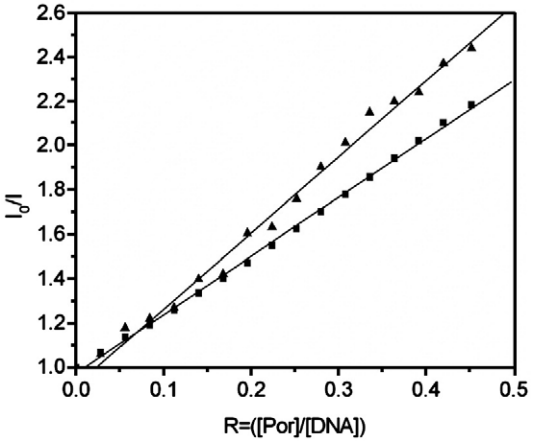


Fig. 7. Florescence quenching curves of DNA-bound EB by [AQATMPyP]$I_3$ (■) and [HTMPyP]$I_3$ (▲) in Tris buffer (pH=7.2, 0.05 M NaCl). ([DNA]=100 μM, [EB]=16.0 μM, $\lambda_{ex}$=537 nm).

Such a result can not be simply explained by the partial intercalation of anthraquinone moiety to DNA, but can be reasonably explained with the combined mode of outside binding (for porphyrin moiety) and partial intercalation (for anthraquinone moiety). When anthraquinone moiety partially intercalates into DNA base pairs, the simultaneous outside binding of porphyrin moiety must be helpful to bend (or kink) the DNA helix and thus reduce the DNA length rapidly. Therefore, the interesting viscosity experiment further confirms the suggestion of the interaction of [AQATMPyP]$I_3$ with DNA in a combined mode of outside binding and partial interaction.

In addition, attempts to see the DNA viscosity change in higher [Por]/[DNA] ratios for [AQATMPyP]$I_3$ can not be successful because red precipitations were observed visually under these conditions. Similar phenomena were observed by Hoffman and Kang, respectively [47,48]. They ascribed these phenomena to the external binding mode between the positive macrocycles and the negative phosphate backbone. Similarly, the appearance of the precipitations in our viscosity experiment may also indicate that the porphyrin moiety of the hybrid, which has positive pyridine rings, probably facilitate outside binding with the DNA phosphate groups through electrostatic interaction.

### 3.1.5. Competitive binding experiments

The above experimental results suggest that there are some interactions between the two compounds and DNA. In order to compare quantitatively, the binding affinities of [AQATMPyP]$I_3$ and [HTMPyP]$I_3$, their $K_{app}$ to CT DNA have to be measured. UV–Vis titration has been used to determine $K_{app}$ of cationic porphyrins for CT DNA [49,50]. However, this method has two severe limitations: (1) it is difficult to determine the absorption coefficient of bound porphyrin; (2) it is only applicable to intercalating porphyrins for which the Soret band is greatly modified upon binding to DNA [51]. In order to avoid these limits, fluorescence spectrum was used to measure $K_{app}$ by competition between EB and the studied compound for binding to DNA. This method measures the decrease of

Table 1
Energies ($\varepsilon_i$/eV) of some frontier molecular orbitals of DNA and $[AQATMPyP]^{3+}$, $[HTMPyP]^{3+}$

| Compound | HOMO−5 | HOMO−4 | HOMO−3 | HOMO−2 | HOMO−1 | HOMO | LUMO | LUMO+1 |
|---|---|---|---|---|---|---|---|---|
| DNA [a] | −2.06 | −1.98 | −1.79 | −1.69 | −1.33 | −1.27 | | |
| $[AQATMPyP]^{3+}$ [b] | −11.95 | −11.78 | −11.71 | −11.58 | −11.1 | −10.99 | −9.25 | −9.24 |
| $[HTMPyP]^{3+}$ [b] | −12.95 | −12.61 | −12.29 | −11.9 | −11.88 | −11.17 | −9.45 | −9.32 |
| Compound | LUMO+2 | LUMO+3 | LUMO+4 | LUMO+5 | LUMO+6 | LUMO+7 | LUMO+8 | LUMO+9 |
| $[AQATMPyP]^{3+}$ [b] | −8.68 | −8.45 | −8.27 | −7.9 | −7.88 | −7.83 | −7.48 | −7.01 |
| $[HTMPyP]^{3+}$ [b] | −8.91 | −8.54 | −8.41 | −7.96 | −7.92 | −7.89 | −7.12 | −5.45 |

[a] The data of DNA are from Ref. [25].
[b] Calculated with B3lYP/6-31G method.

fluorescence of EB bound to DNA in the presence of the compound of interest. It can be used for all compounds having a good affinity for DNA whatever their binding modes may be because it only measures the ability of a compound to prevent intercalation of EB into DNA [4].

The EB competitive binding experiments were carried out and quenching plot are given in Fig. 7. The quenching plot of $I_0$/I *vs.* [Por]/[DNA] is in good agreement with the linear Stern–Volmer equation with a slope of 2.58, 3.26, for $[AQATMPyP]I_3$ and $[HTMPyP]I_3$, respectively. We can also learn from Fig. 7 that 50% of EB molecules were replaced from DNA-bound EB at a concentration ratio of [Por]/[EB]=2.91, 2.3 for $[AQATMPyP]I_3$ and $[HTMPyP]I_3$, respectively. By taking $K_{app}$ of $1.0\times10^7$ $M^{-1}$ for EB under this experimental condition [52], the $K_{app}$ of $[AQATMPyP]I_3$ and $[HTMPyP]I_3$ were derived $3.44\times10^6$ $M^{-1}$ and $4.35\times10^6$ $M^{-1}$ ($K_{app}$(EB)/2.91, $K_{app}$(EB)/2.3), respectively [53]. The DNA binding affinity of the Por-AQ hybrid is a little weaker than its parent porphyrin. This may also result from the severe steric hindrance between the two moieties in the hybrid.

### 3.1.6. Theoretical explanation

Frontier molecular orbital theory [54] was used to explain the DNA binding behaviors of $[AQATMPyP]^{3+}$ and $[HTMPyP]^{3+}$. Table 1 gives the energies of some frontier molecular orbitals of DNA [25] and the two compounds. Obviously, the energies of the HOMO and HOMO−$x$ ($x$=1–6) of DNA base pairs are all much higher than those of the LUMO and LUMO+$x$ ($x$=1–9) of $[AQATMPyP]^{3+}$ and $[HTMPyP]^{3+}$. Therefore, when bind to DNA, the two compounds will be good electron acceptors and DNA will be good electron donors [25,54,55,56].

From the optimized geometrical structures (Fig. 8) and geometric parameters (Table 2), the anthraquinone plane and porphyrin plane of $[AQATMPyP]^{3+}$ are almost vertical to each

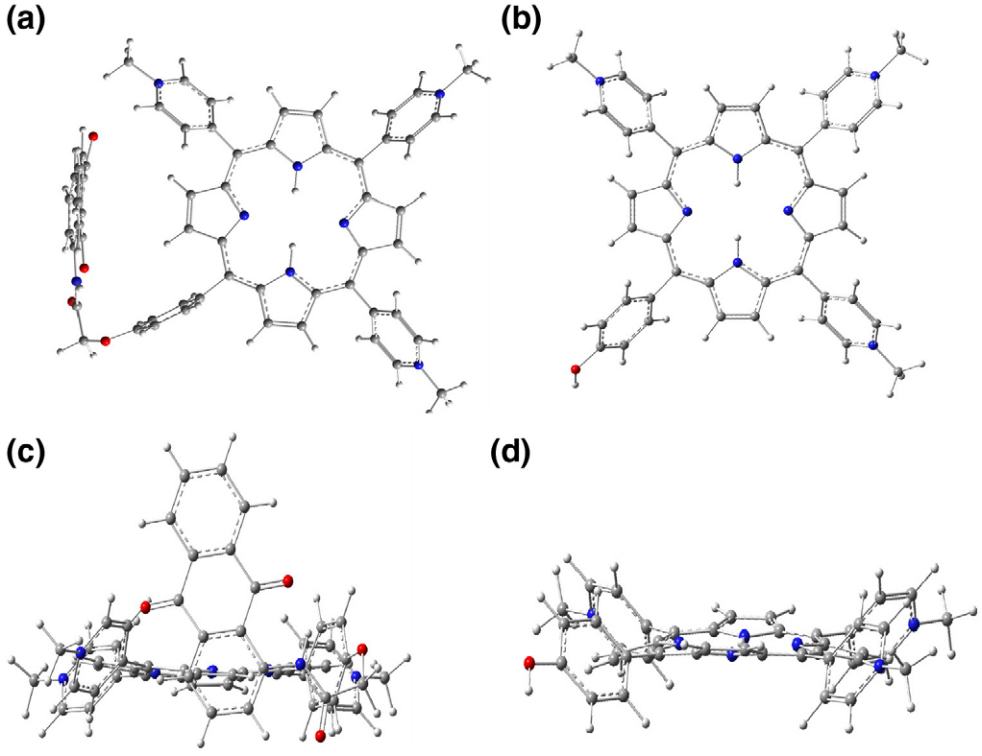


Fig. 8. Optimized structures of $[AQATMPyP]^{3+}$, top view (a); $[HTMPyP]^{3+}$, top view (b); $[AQATMPyP]^{3+}$, side view (c); $[HTMPyP]^{3+}$, side view (d).

Table 2
Selective dihedral angles (in °) and distances (in nm) for $[AQATMPyP]^{3+}$ and $[HTMPyP]^{3+}$

| Compound[a] | $N_1–N_2–N_3–N_4$ | $N_1–C_5–C_6–C_7$ | $C_9–C_8–C_6–C_5$ | $O_{12}–C_{11}–C_{10}–C_9$ | $C_{14}–C_{13}–C_{12}–O_{11}$ | $N_{15}–C_{14}–C_{13}–C_{12}$ | $C_{16}–C_{15}–N_{14}–C_{13}$ |
|---|---|---|---|---|---|---|---|
| $AQATMPyP]^{3+}$ | 0.09 | 2.86 | 77.33 | −172.50 | −61.73 | −31.94 | 172.43 |
| $[HTMPyP]^{3+}$ | 1.95 | −7.86 | −54.61 | −179.34 | | | |

| Compound[a] | $C_{18}–C_{17}–C_{16}–N_{17}$ | $O_{19}–C_{18}–C_{17}–C_{16}$ | $N_1–N_2–C_{16}–C_{21}$ | $N_1–N_2–C_{16}–C_{18}$ | $O_{19}–C_6$ | $N–O_{22}$[b] | $H–O_{22}$[b] |
|---|---|---|---|---|---|---|---|
| $[AQATMPyP]^{3+}$ | −5.57 | 6.63 | −175.59 | 92.2 | 0.6143 | 0.3571 | 0.2694 |

[a] The corresponding atomic labels are seen in Fig. 1.
[b] The smallest distance between the N (H) atom of methyl pyridine and the O atom of anthraquinone.

other (the dihedral angle $N_1–N_2–C_{16}–C_{18}$ is 92.2°). Meanwhile, the nearest distance between N (H) atom of methyl pyridine group and the O atom of the anthraquinone is 0.3571 nm (0.2694 nm). Thus, there must be severe steric hindrance for either plane to fully intercalate in DNA. Although the anthraquinone moiety has good planarity (the related dihedral angle of $O_{19}–C_{18}–C_{17}–C_{16}$ is 6.63°) and LUMO+6 mainly distributes on anthraquinone moiety (see Fig. 9a, the contour plots of some frontier MOs of $[AQATMPyP]^{3+}$), it may only partially intercalate in DNA because of the steric hindrance from the vertical porphyrin plane and methyl pyridine group nearby. Meanwhile, from Fig. 9a we can also find that for

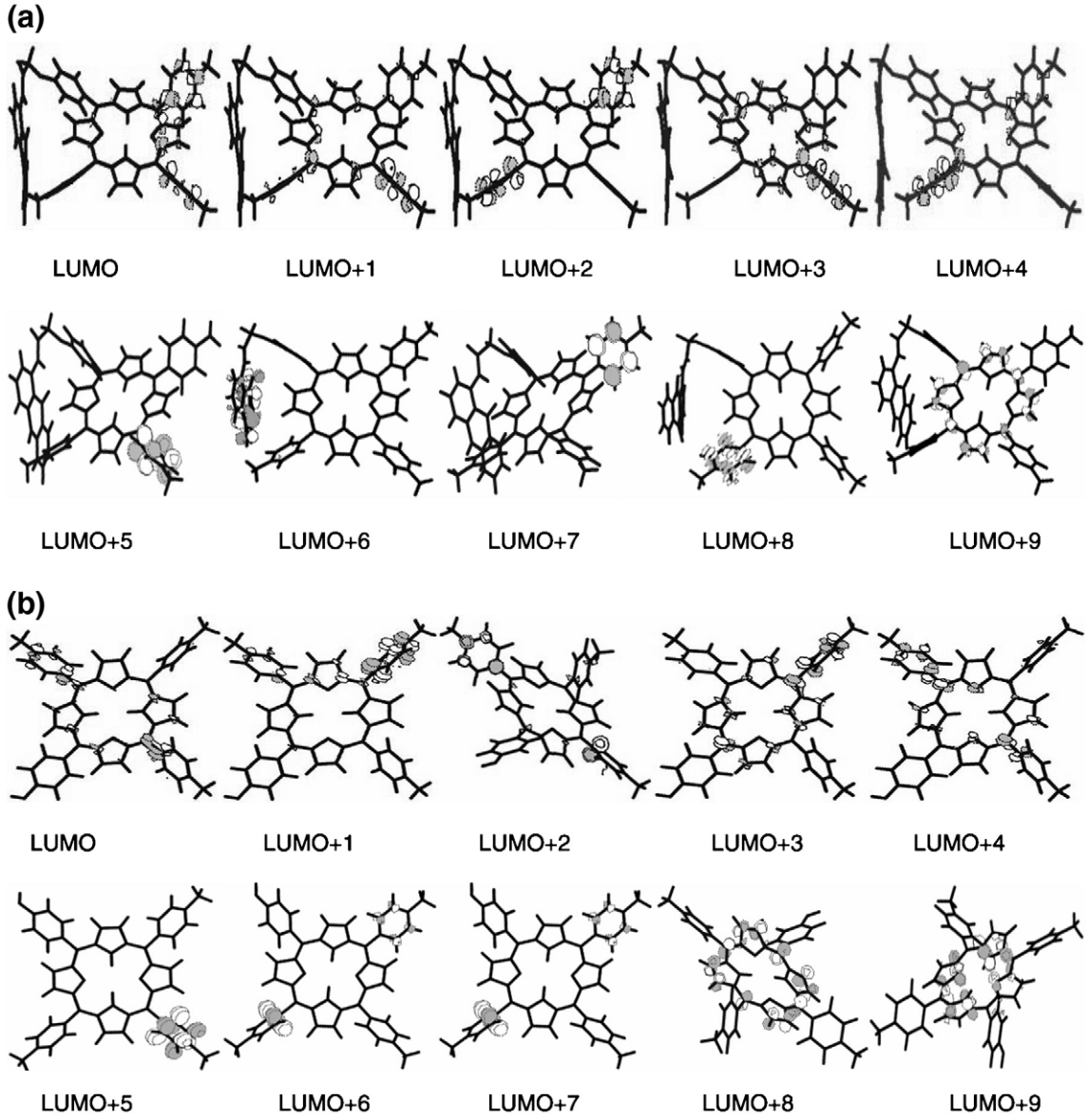


Fig. 9. Some frontier orbital contour maps of $[AQATMPyP]^{3+}$ (a) and $[HTMPyP]^{3+}$ (b) calculated with DFT at B3LYP/6-31G level.

$[AQATMPyP]^{3+}$, the components of LUMO and LUMO+$x$ ($x$=1–5, 7, 8) are mainly from π orbital of pyridine planes. Thus, π–σ orbital stacking of methyl-pyridine groups and phosphate groups ($-PO_4^{3-}$) of DNA may be feasible while the π–π stacking interaction of porphyrin core with DNA base pairs may be relatively difficult. Because of the severe steric hindrance from anthraquinone and disadvantageous population of LUMO, the cationic porphyrin moiety of $[AQATMPyP]^{3+}$ probably couldn't intercalate in DNA but may interact via electrostatic effect between positive methyl-pyridine groups and negative DNA backbone.

In the case of $[HTMPyP]^{3+}$, the porphyrin plane has excellent planarity (the dihedral angle $N_1$–$N_2$–$N_3$–$N_4$ is 1.95°) just as the classical DNA intercalative reagent TMPyP does [4]. Meanwhile, Fig. 9b shows that for $[HTMPyP]^{3+}$, LUMO+3, LUMO+8 and LUMO+9 mostly distribute on the porphyrin core. Since there is no steric hindrance from other moieties and the π–π stacking interaction of porphyrin core with DNA base pairs are of large orbital stacking and stronger than the electrostatic interaction via small π–σ orbital stacking of methyl-pyridine groups and $-PO_4^{3-}$ of DNA, $[HTMPyP]^{3+}$ may mainly bind to DNA in a classic intercalative mode.

The large $K_{app}$ of $[AQATMPyP]^{3+}$ for DNA can be assigned to the conjunct effect of intercalation via anthraquinone moiety and electrostatic interaction via porphyrin moiety, and the large $K_{app}$ of $[HTMPyP]^{3+}$ can be assigned to the intercalative binding mode via large porphyrin plane and its high withdrawing electron ability induced by three positive methyl-pyridine groups. The effective stacking between the porphyrin core of $[HTMPyP]^{3+}$ and the DNA base pairs is likely to be the main reason that its $K_{app}$ is slightly larger than that of $[AQATMPyP]^{3+}$.

The above theoretical results can explain the DNA-binding properties of the two compounds to a certain extent. However, our theoretical calculation skill is not so mature and needs further development. For example, modeling of the large DNA-porphyrin-antraquinone systems with molecular mechanics method instead of modeling isolated compounds with quantum chemistry method would provide valuable information for such kind of studies. We are trying our best to attempt such project currently.

### 3.2. DNA photocleavage

Some porphyrins have been reported to involve a $^1O_2$ mediated mechanism in DNA photocleavage [57–59]. In order to establish the reactive species responsible for the DNA photocleavage by the porphyrin chromophore in the two compounds, we investigated the influence of different potentially inhibiting agents. Yellow light filter ($\lambda$>470 nm) was used in the high pressure mercury lamp to keep the lamp's emission wavelength in the visible range (porphyrin's absorption) [60]. In the case of $[AQATMPyP]I_3$ (Fig. 10a), study with $NaN_3$, a $^1O_2$ quencher [14], was carried out and the plasmid cleavage was significantly inhibited (lane 2). The photocleavage efficiency was also greatly inhibited when irradiation reaction was done under an Ar atmosphere (lane 3). On the other hand, the photocleavage ability was enhanced by replacing the reaction

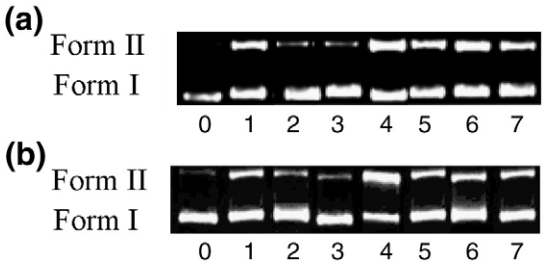


Fig. 10. Photocleavage of pBR322 DNA in the presence of $[AQATMPyP]I_3$ (a) or $[HTMPyP]I_3$ (b) and different inhibitors after irradiation by visible light ($\lambda$>470 nm)for 20 min. 10 μL reaction mixtures contained 1.0 μg of plasmid DNA. [Por]=2 μM. Lane 0: DNA control; lane 1: in the presence of porphyrin, no inhibitor; lanes 2–6: in the presence of porphyrin and inhibitor, (2) $NaN_3$ (5 mM), (3) under an Ar atmosphere, (4) 70%$D_2O$, (5) ethanol (5 mM), (6) methanol (5 mM), (7) DMSO (5 mM).

media $H_2O$ by 70% $D_2O$ which makes the life span of $^1O_2$ longer (lane 4). These results suggest that $^1O_2$ is likely to be one of the reactive species responsible for the cleavage reaction. Meanwhile, the cleavage of the plasmid was not inhibited in the presence of hydroxyl radical ($OH^{\cdot}$) scavengers such as ethanol (lane 5), methanol (lane 6) and DMSO (lane 7) even at high concentration, suggesting that hydroxyl radical may not be the cleaving agent. Similar cases have also been observed for $[HTMPyP]I_3$ under identical conditions (Fig. 10b).

It has been frequently reported that the excited quinone compounds are powerful oxidants and some of them can cleavage DNA through oxidate guanine (G) of DNA [61–64]. Thermodynamic considerations play a key role in assessing the likelihood that excited quinone compounds will react with DNA by electron transfer. Weller equation [65] is widely used to determine whether this reaction is feasible [62–64]:

$$\Delta G_{et} = E^{+}_{D/D} - E^{-}_{A/A} - \Delta E_{0,0}$$

The oxidation potentials of the nucleic acid bases have been determined previously [66]. The oxidation potential of isolated $G$ ($E^{+}_{D/D}$) is 1.29 V (*vs.* NHE) and this value will be much lower for the stacking $G$ in DNA [67–69]. The reduction potential of $[AQATMPyP]I_3$ ($E^{-}_{A/A}$) was determined to be −0.36 V (NHE) using CV method. The $\Delta E_{0,0}$ energy of $[AQATMPyP]I_3$ was determined to be 1.90 eV approximately, from its maximum emission wavelength [70]. $\Delta G_{et}$ is thus calculated to be −0.25 eV according to the Weller equation, revealing that electron transfer from guanine of DNA to excited $[AQATMPyP]I_3$ is exothermic and therefore feasible on thermodynamic grounds.

A wavelength dependent photocleavage of some non-charged Por-AQ hybrids to DNA has been reported by Goverdhan Mehta and his coworkers [21]. They have found that those hybrids show high photocleavage efficiency at anthraquinone's absorption and minor efficiency at porphyrin's absorption, and thus have concluded that the anthraquinone moiety intercalates in DNA and the non-charged porphyrin moiety situated away from the duplex. We have also previously reported the DNA photocleavage activity of some neutral Por-AQ hybrids and have got similar experimental results as Goverdhan's [22].

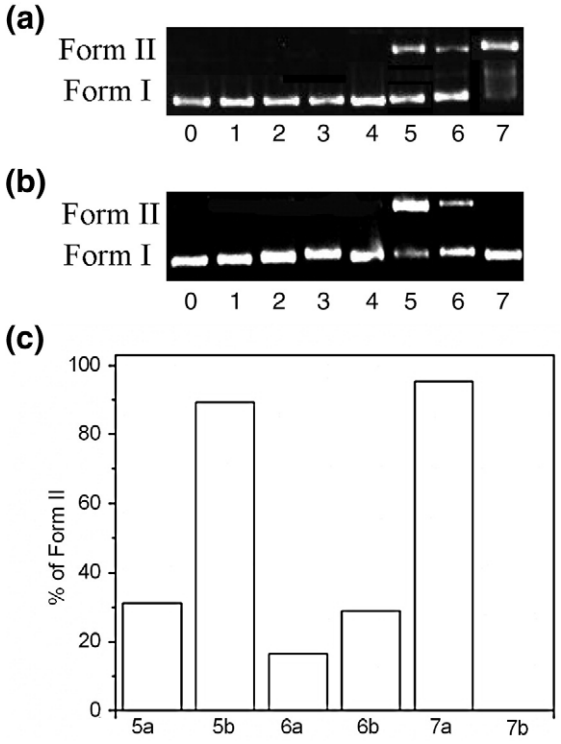


Fig. 11. Photocleavage plasmid of pBR322 DNA after irradiated by visible light ($\lambda$>470 nm) (a) or ultraviolet light ($\lambda$<350 nm), under an Ar atmosphere (b) and the percentage of DNA in Form II for lanes 5, 6 and 7 (c). 10 μL reaction mixtures contained 1.0 μg of plasmid DNA. [Por]=2 μM. Lane 0: untreated DNA, no irradiation; Lane 1, 2, 3: in the presence of $[AQATMPyP]I_3$, AQATPP, $[HTMPyP]I_3$, respectively, no irradiation; Lane 4: untreated DNA, irradiation for 25 min; Lane 5, 6, 7: in the presence of $[AQATMPyP]I_3$, AQATPP, $[HTMPyP]I_3$, respectively, irradiation for 25 min.

Herein, in order to better understand the DNA photocleavage of the studied cationic Por-AQ hybrid, a non-charged Por-AQ hybrid, AQATPP was comparably investigated. Fig. 11 gives the experimental results of wavelength-depending DNA photocleavage of $[AQATMPyP]I_3$, AQATPP and $[HTMPyP]I_3$. No DNA cleavage is observed for the control in which compounds were absent (lane 0), or incubation of the plasmid DNA with the compounds in the dark (lane 1, 2, 3). In Fig. 11a, when irradiated at porphyrin's absorption ($\lambda$>470 nm), the photocleavage ability order of the three compounds is $[HTMPyP]I_3$ (95.4%)>$[AQATMPyP]I_3$ (31.2%)>AQATPP(16.5%). This may relate to the different binding situation of porphyrin moiety to DNA. $[HTMPyP]I_3$ intercalates into the DNA duplex and the porphyrin moiety in $[AQATMPyP]I_3$ binds to DNA with outside binding mode which is less advantageous in DNA interaction, while the non-charged porphyrin moiety in AQATPP situates away from the DNA duplex [21,22]. On the other hand, when irradiated at anthraquinone's absorption ($\lambda$<350 nm) and under an Ar atmosphere, the photocleavage abilities of the compounds follow the order of $[AQATMPyP]I_3$ (89.3%)>AQATPP (28.9%)>$[HTMPyP]I_3$ (0). The cationic porphyrin $[HTMPyP]I_3$ can not cleavage DNA under this condition, which may because of the lack of $O_2$ in the Ar atmosphere. Thus, the DNA cleavage ability of the two hybrids can only attribute to the excited anthraquinone moiety [21]. From the foregoing analysis, anthraquinone moiety in $[AQATMPyP]I_3$ partially intercalates into DNA and completely intercalates into DNA in AQATPP [21,22]. From the point of binding mode, $[AQATMPyP]I_3$ is less advantageous in DNA photocleavage. However, $[AQATMPyP]I_3$ has higher cleavage efficiency than AQATPP under this condition. This may be mainly attributed to the much higher DNA binding ability of the cationic Por-AQ hybrid than the neutral one. The anthraquinone moiety in $[AQATMPyP]I_3$ has more chances to approach the negative DNA unit, and thus has more opportunities to oxidate DNA bases. The wavelength dependent photocleavage experiment here proves that the cleavage behaviors of the compounds are closely related to their DNA binding behaviors [14,21].

## 4. Conclusions

A novel cationic Por-AQ hybrid $[AQATMPyP]I_3$ and its parent porphyrin $[HTMPyP]I_3$ were synthesized and characterized. The results of absorption, fluorescence and CD spectra as well as viscosity measurements suggest that, in low [Por]/[AQ] ratios, the $[HTMPyP]I_3$ binds to DNA in an intercalative mode while the hybrid $[AQATMPyP]I_3$ binds to DNA in a combined mode of a partial intercalative binding mode (via anthraquinone plane) and an outside binding mode (via the positive porphyrin moiety). The theoretical calculations applying DFT have been carried out and the calculational results can reasonably explain the experimental findings above. In addition, $^1O_2$ is suggested to be the reactive species responsible for the photocleavage reaction of both $[AQATMPyP]I_3$ and $[HTMPyP]I_3$ under irradiation at porphyrin's excitation wavelength and electron transfer occurs from the DNA bases to $[AQATMPyP]I_3$ under irradiation at anthraquinone's excitation wavelength. The DNA photocleavage behaviors of the compounds were consistent with their DNA binding properties and $[AQATMPyP]I_3$ exhibits wavelength-depending photocleavage ability.

## Acknowledgements

We are grateful to the supports of Guangzhou Municipality Science & Technology Bureau of China, the National Natural Science Foundation of China and National Key Foundation Research Development Project (973) Item of China (No. 2007 CB815306).

## References

[1] T.J. Dougherty, Y. Hayata, Autoradiographic distribution of hematoporphyrin derivative in normal and tumor tissue of the mouse, Cancer Res. 41 (1981) 4606–4612.
[2] B. Armitage, Photocleavage of nucleic acids, Chem. Rev. 98 (1998) 1171–1200.
[3] R.J. Fiel, B.R. Munson, Binding of meso-tetra (4-*N*-methylpyridyl) porphine to DNA, Nucleic Acids Res. 8 (1980) 2835–2842.
[4] R.F. Pasternack, E.J. Gibbs, J.J. Villafranca, Interactions of porphyrins with nucleic acids, Biochemistry 22 (1983) 2406–2414.
[5] N.E. Mukundan, G. Pethd, D.W. Dixon, L.G. Marzill, DNA-tentacle porphyrin interactions: at over GC selectivity exhibited by an outside binding self-stacking porphyrin, Inorg. Chem. 34 (1995) 3677–3687.

[6] R.T. Wheelhouse, D. Sun, H. Han, F.X. Han, L.H. Hurley, Cationic porphyrins as telomerase inhibitors: the interaction of tetra-(*N*-methyl-4-pyridyl)porphine with quadruplex DNA, J. Am. Chem. Soc. 120 (1998) 3261–3262.
[7] N.R. Barnes, A.F. Schreiner, B-DNA binding with cobalt(III) and vanadyl (2+) derivatives of tetracationic 5,10,15,20-tetrakis(4-*N*-methylpyridyl) porphine: combined CD, optical, and electronic MCD spectra, Inorg. Chem. 37 (1998) 6935–6938.
[8] D.R. McMillin, K.M. McNett, Photoprocesses of copper complexes that bind to DNA, Chem. Rev. 98 (1998) 1201–1220.
[9] S.Y. Rha, E. Izbicka, R. Lawrence, K. Davidson, D. Sun, M.P. Moyer, G.D. Roodman, L.H. Hurley, D.D. Von Hoff, Effect of telomere and telomerase interactive agents on human tumor and normal cell lines, Clin. Cancer Res. 6 (2000) 987–993.
[10] R.K. Wall, A.H. Shelton, D.R. McMillin, $H_2$D3: a cationic porphyrin designed to intercalate into B-form DNA ($H_2$D3=*trans*-Di(*N*-methylpyridium-3-yl)porphyrin), J. Am. Chem. Soc. 123 (2001) 11480–11481.
[11] D.R. McMillin, A.H. Shelton, S.A. Bejune, P.E. Fanwick, R.K. Wall, Understanding binding interactions of cationic porphyrins with B-form DNA, Coord. Chem. Rev. 249 (2005) 1451–1459.
[12] H. Li, O.S. Fedorova, R.W. Trumble, T.R. Fletcher, Site-specific photomodification of DNA by porphyrin-oligonucleotide conjugates synthesized via a solid phase H-phosphonate Approach, Bioconjug. Chem. 8 (1997) 49–56.
[13] Y. Ishikawa, A. Yamashita, T. Uno, Efficient photocleavage of DNA by cationic porphyrin-acridine hybrids with the effective length of diamino alkyl linkage, Chem. Pharm. Bull. 49 (2001) 287–293.
[14] T. Jia, Z.X. Jiang, K. Wang, Z.Y. Li, Binding and photocleavage of cationic porphyrin-phenylpiperazine hybrids to DNA, Biophys. Chemist. 119 (2006) 295–302.
[15] B. Armitage, C.J. Yu, C. Devadoss, G.B. Schuster, Cationic anthraquinone derivatives as catalytic DNA photonucleases: mechanisms for DNA damage and quinone recycling, J. Am. Chem. Soc. 116 (1994) 9847–9859.
[16] D.T. Breslin, J.E. Coury, J.R. Anderson, L. Mcfail-Isom, Y. Kan, L.D. Williams, L.A. Bottomley, G.B. Schuster, Anthraquinone photonuclease structure determines its mode of binding to DNA and the cleavage chemistry observed, J. Am. Chem. Soc. 119 (1997) 5043–5044.
[17] R.E. McKnight, J.G. Zhang, D.W. Dixon, Binding of a homologous series of anthraquinones to DNA, Bioorg. Med. Chem. Lett. 14 (2004) 401–404.
[18] J.M. Sessler, M.R. Johnson, The synthesis of 1, 3- and 1, 4-phenylene-linked bisquinone-substituted porphyrin dimers, Angew. Chem., Int. Ed. Engl. 26 (1987) 678–680.
[19] A. Osuka, S. Morikawa, K. Maruyama, S. Hirayama, T. Minami, An efficient photochemical synthesis of conformationally restricted quinone-substituted porphyrins, J. Chem. Soc., Chem. Commun. 5 (1987) 359–361.
[20] A. Osuka, K. Maruyama, S. Hirayama, Quinone-linked and quinone-capped porphyrins. Their one-pot photochemical synthesis and fluorescence behavior, Tetrahedron 45 (1989) 4815–4829.
[21] G. Mehta, S. Muthusamy, B.G. Maiya, S. Arounaguiri, Porphyrin-anthraquinone hybrids: wavelength dependent DNA photonucleases, Tetrahedron Lett. 38 (1997) 7125–7128.
[22] L. Ma, J.Z. Lu, L.F. Fan, J.W. Huang, L.N. Ji, DNA-photocleavage of a porphyrin-anthraquinone hybride, Acta Sci. Nat. Unvis. Sun Yet-Seni. 42 (2003) 129–131.
[23] A.D. Becke, Density-functional exchange-energy approximation with correct asymptotic behavior, Phys. Rev., A 38 (1988) 3098–3100.
[24] J.P. Perdew, Density-functional approximation for the correlation energy of the inhomogeneous electron gas, Phys. Rev., B 33 (1986) 8822–8824.
[25] N. Kurita, K. Kobayashi, Density functional MO calculation for stacked DNA base pairs with backbones, Comput. Chem. 24 (2000) 351–357.
[26] K.C. Zheng, J.P. Wang, W.L. Peng, X.W. Liu, F.C. Yun, Studies on 6,6′-disubstitution effects of the dpq in $[Ru(bpy)_2(dpq)]^{2+}$ with DFT method, J. Phys. Chem., A 105 (2001) 10899–10905.
[27] H. Xu, K.C. Zheng, H. Deng, L.J. Lin, Q.L. Zhang, L.N. Ji, Effects of the ancillary ligands of polypyridyl ruthenium(II) complexes on the DNA-binding behaviors, New J. Chem. 27 (2003) 1255–1263.
[28] L.C. Xu, J. Li, Y. Shen, K.C. Zheng, L.N. Ji, Theoretical studies on the excited states, DNA photocleavage, and spectral properties of complex $[Ru(phen)2(6\text{-}OH\text{-}dppz)]^{2+}$, J. Phys. Chem., A 111 (2007) 273–280.
[29] J. Li, J.C. Chen, L.C. Xu, K.C. Zheng, L.N. Ji, A DFT/TDDFT study on the structures, trend in DNA-binding and spectral properties of molecular ''light switch''complexes [Ru(phen)2(L)]2+(L=dppz, taptp, phehat), J. Organomet. Chem. 692 (2007) 831–838.
[30] P.J. Walsh, K.C. Gordon, D.L. Officer, W.M. Campbell, A DFT study of the optical properties of substituted Zn(II)TPP complexes, J. Mol. Struct., Theochem 759 (2006) 17–24.
[31] Z.Y. Li, H.L. Wang, T.T. Lu, T.J. He, F.C. Liu, D.M. Chen, Density functional theory studies on the electronic and vibrational spectra of octaethylporphyrin diacid, Spectrochim. Acta, Part A 67 (2007) 1382–1391.
[32] C. Casas, B. Saint-Jalmes, C. Loup, C.J. Lacey, Bernard Meunier, Synthesis of cationic metalloporphyrin precursors related to the design of DNA cleavers, J. Org. Chem. 58 (1993) 2913–2917.
[33] M.E. Reichmann, S.A. Rice, C.A. Thomas, P. Doty, A further examination of the molecular weight and size of desoxypentose nucleic acid, J. Am. Chem. Soc. 76 (1954) 3047–3053.
[34] G. Schaftenaar, Molden V4.2 Program CAOS/CAMM Center Nijmegen Toernooiveld, Nijmegen, The Netherlands, 1991.
[35] M.J. Frisch, G.W. Trucks, H.B. Schlegel, G.E. Scuseria, M.A. Robb, J.R. Cheeseman, J.A. Montgomery, T. Vreven Jr., K.N. Kudin, J.C. Burant, J.M. Millam, S.S. Iyengar, J. Tomasi, V. Barone, B. Mennucci, M. Cossi, G. Scalmani, N. Rega, G.A. Petersson, H. Nakatsuji, M. Hada, M. Ehara, K. Toyota, R. Fukuda, J. Hasegawa, M. Ishida, T. Nakajima, Y. Honda, O. Kitao, H. Nakai, M. Klene, X. Li, J.E. Knox, H.P. Hratchian, J.B. Cross, V. Bakken, C. Adamo, J. Jaramillo, R. Gomperts, R.E. Stratmann, O. Yazyev, A.J. Austin, R. Cammi, C. Pomelli, J.W. Ochterski, P.Y. Ayala, K. Morokuma, G.A. Voth, P. Salvador, J.J. Dannenberg, V.G. Zakrzewski, S. Dapprich, A.D. Daniels, M.C. Strain, O. Farkas, D.K. Malick, A.D. Rabuck, K. Raghavachari, J.B. Foresman, J.V. Ortiz, Q. Cui, A.G. Baboul, S. Clifford, J. Cioslowski, B.B. Stefanov, G. Liu, A. Liashenko, P. Piskorz, I. Komaromi, R.L. Martin, D.J. Fox, T. Keith, M.A. Al-Laham, C.Y. Peng, A. Nanayakkara, M. Challacombe, P.M.W. Gill, B. Johnson, W. Chen, M.W. Wong, C. Gonzalez, J.A. Pople, Gaussian 03, Revision D.01, Gaussian, Inc., Wallingford CT, 2005.
[36] H.Y. Liu, J.W. Huang, X. Tian, X.D. Jiao, G.T. Luo, L.N. Ji, Chiral linear assembly of amino acid bridged dimeric porphyrin hosts, Chem. Commun. 17 (1997) 1575–1576.
[37] R.J. Fiel, J.C. Howard, E.H. Mark, N. Datta-Gupta, Interaction of DNA with a porphyrin ligand: evidence for intercalation, Nucleic Acids Res. 6 (1979) 3093–3100.
[38] D.H. Tjahjono, S. Mima, T. Akutsu, N. Yoshioka, H. Inoue, Interaction of metallopyrazoliumylporphyrins with calf thymus DNA, J. Inorg. Biochem. 85 (2001) 219–228.
[39] M.R. Wasielewski, Photoinduced electron transfer in supramolecular systems for artificial photosynthesis, Chem. Rev. 92 (1992) 435–461.
[40] L.N. Ji, X.H. Zou, J.G. Liu, Shape and enantioselective interaction of Ru(II)/Co(III) polypyridyl complexes with DNA, Coord. Chem. Rev. 216–217 (2001) 513–536.
[41] E. Nyarko, N. Hanada, A. Habib, M. Tabata, Fluorescence and phosphorescence spectra of Au(III), Pt(II) and Pd(II) porphyrins with DNA at room temperature, Inorg. Chim. Acta 357 (2004) 739–745.
[42] T. Masaaki, K.S. Ashish, N. Elvis, Enhanced conformational changes in DNA in the presence of mercury(II), cadmium(II) and lead(II) porphyrins, J. Inorg. Biochem. 94 (2003) 50–58.
[43] N.E. Mukundan, G. Petho, D.W. Dixon, M.S. Kim, L.G. Marzilli, Interactions of an electron-rich tetracationic tentacle porphyrin with calf thymus DNA, Inorg. Chem. 33 (1994) 4676–4687.
[44] C.V. Kumar, J.K. Barton, N.J. Turro, Photophysics of ruthenium complexes bound to double helical DNA, J. Am. Chem. Soc. 107 (1985) 5518–5523.
[45] S. Satyanarayana, J.C. Dabrowiak, J.B. Chaires, Neither Δ- nor λ-tris (phenanthroline)ruthenium(II) binds to DNA by classical intercalation, Biochemistry 31 (1992) 9319–9324.
[46] S. Satyanaryana, J.C. Daborusak, J.B. Chaires, Tris(phenanthroline) ruthenium(II) enantiomer interactions with DNA: mode and specificity of binding, Biochemistry 32 (1993) 2573–2584.
[47] E.A. Maírín, G.M. Barrett, M.H. Brian, Binding of octa-plus porphyrazines to DNA, J. Inorg. Biochem. 80 (2000) 257–260.

[48] J.W. Kang, H.X. Wu, X.Q. Lu, Y.S. Wang, L. Zhou, Study on the interaction of new water-soluble porphyrin with DNA, Spectrochim. Acta, Part A 61 (2005) 2041–2047.
[49] R.J. Fiel, J.C. Howard, E.H. Mark, N.D. Gupta, Interaction of DNA with a porphyrin ligand: evidence for intercalation, Nucleic Acids Res. 6 (1979) 3093–3118.
[50] G. Dougherty, J.R. Pilbrow, A. Skorobogaty, T.D. Smith, Electron spin resonance spectroscopic and spectrophotometric investigation of the binding of tetracationic porphyrins and porphyrazines with calf thymus DNA, J. Chem. Soc., Faraday Trans. 2 (81) (1985) 1739–1759.
[51] M.A. Sari, J.P. Battioni, D. Dupre, D. Mansuy, J.B. Lepecq, Interaction of cationic porphyrins with DNA: importance of the number and position of the charges and minimum structural requirements for intercalation, Biochemistry 29 (1990) 4205–4215.
[52] Y.Y. Fang, B.D. Ray, C.A. Caussen, K.B. Lipkowitz, E.C. Long, Ni (II)·Arg-Gly-His-DNA interactions: investigation into the basis for minor-groove binding and recognition, J. Am. Chem. Soc. 126 (2004) 5403–5412.
[53] M.J. Han, L.H. Gao, Y.Y. Lu, K.Z. Wang, Ruthenium(II) complex of Hbopip: synthesis, characterization, pH-induced luminescence "Off-On-Off" switch, and avid binding to DNA, J. Phys. Chem., B 110 (2006) 2364–2371.
[54] G. Klopman, Chemical reactivity and the concept of charge-and frontier-controlled reactions, J. Am. Chem. Soc. 90 (1968) 223–234.
[55] I. Fleming, Frontier Orbital and Organic Chemical Reaction, Wiley, New York, 1976.
[56] D. Řeha, M. Kabeláček, F. Ryjáček, J. Šponer, J.E. Šponer, M. Elstner, S. Suhai, P. Hobza, Intercalators. 1. Nature of stacking interactions between intercalators (Ethidium, daunomycin, ellipticine, and 4′,6-Diaminide-2-phenylindole) and DNA base pairs. ab Initio quantum chemical, density functional theory, and empirical potential study, J. Am. Chem. Soc. 124 (2002) 3366–3376.
[57] J.D. Thomas, J.G. Charles, W.H. Barbara, J. Giulio, K. David, K. Mladen, M. Johan, P. Qian, Photodynamic Therapy, J. Natl. Cancer Inst. 90 (1998) 889–905.
[58] E.D. Sternberg, D. Dolphin, C. Bruckner, Porphyrin-based photosensitizers for use in photodynamic therapy, Tetrahedron 54 (1998) 4151–4202.
[59] R. Bonnett, Chemical Aspects of Photodynamic Therapy, Gordon and Breach Science, Amsterdam, 2000.
[60] C.J. Sansonetti, M.L. Salit, J. Reader, Wavelengths of spectral lines in mercury pencil lamps, Appl. Opt. 35 (1996) 74–77.
[61] B. Armitage, C. Yu, C. Devadoss, G.B. Schuster, Cationic anthraquinone derivatives as catalytic DNA photonucleases: mechanisms for DNA damage and quinone recycling, J. Am. Chem. Soc. 116 (1994) 9847–9859.
[62] D.T. Breslin, G.B. Schuster, Anthraquinone photonucleases: mechanisms for GG-Selective and nonselective cleavage of double-stranded DNA, J. Am. Chem. Soc. 118 (1996) 2311–2319.
[63] I. Siato, M. Takayama, H. Sugiyama, K. Nakatani, Photoinduced DNA cleavage via electron transfer: demonstration that guanine residues located 5′ to guanine are the most electron-donating sites, J. Am. Chem. Soc. 117 (1995) 6406–6407.
[64] I. Siato, M. Takayama, Photoactivatable DNA-cleaving amino acids: highly sequence-selective DNA photocleavage by novel L-lysine derivatives, J. Am. Chem. Soc. 117 (1995) 5590–5591.
[65] D. Rehm, A. Weller, Isr. J. Chem. 8 (1970) 259–263.
[66] S. Steenken, S.V. Jovanovic, How easily oxidizable is DNA? One-electron reduction potentials of adenosine and guanosine radicals in aqueous solution, J. Am. Chem. Soc. 119 (1997) 617–618.
[67] H. Sugiyama, I. Saito, Theoretical studies of GG-Specific photocleavage of DNA via electron transfer: significant lowering of ionization potential and 5'-Localization of HOMO of stacked GG bases in B-Form DNA, J. Am. Chem. Soc. 118 (1996) 7063–7068.
[68] M.H. Baik, J.S. Silverman, I.V. Yang, P.A. Ropp, V.A. Szalai, W.T. Yang, H.H. Torp, Using density functional theory to design DNA base analogues with low oxidation potentials, J. Phys. Chem., B 105 (2001) 6437–6444.
[69] L.C. Xu, S. Shi, J. Li, S.Y. Liao, K.C. Zheng, L.N. Ji, A combined computational and experimental study on DNA-photocleavage of Ru(II) polypyridyl complexes [Ru(bpy)2(L)]2+ (L=pip, *o*-mopip and *p*-mopip), Dalton Trans. 2 (2008) 291–301.
[70] N.V. Tkachenko, A.Y. Tauber, D. Grandell, P.H. Hynninen, H. Lemmetyinen, Light-induced electron transfer in pyropheophytin-anthraquinone and phytochlorin-anthraquinone dyads: influence of conformational exchange, J. Phys. Chem., A 103 (1999) 3646–3656.